



the society for solid-state  
and electrochemical  
science and technology

Journal of The Electrochemical Society

## The Reversibility of Sodium Insertion in Transition Metal Trisulfides

Margherita Zanini

*J. Electrochem. Soc.* 1985, Volume 132, Issue 3, Pages 588-593.  
doi: 10.1149/1.2113911

---

**Email alerting  
service**

Receive free email alerts when new articles cite this article - sign up in the box at the top right corner of the article or [click here](#)

---

---

To subscribe to *Journal of The Electrochemical Society* go to:  
<http://jes.ecsdl.org/subscriptions>

---

# The Reversibility of Sodium Insertion in Transition Metal Trisulfides

Margherita Zanini

Ford Motor Company, Dearborn, Michigan 48121

## ABSTRACT

The effects produced by the insertion of sodium in the trisulfides of titanium, niobium, and tantalum were investigated by electrochemical techniques. Cyclic voltammetry measurements were carried out in these materials using high-temperature sodium cells which utilize the solid electrolyte  $\beta'$ -alumina. The data demonstrate that  $\text{TiS}_3$  disproportionates into  $\text{TiS}_2$  and sulfur during the first cycle.  $\text{NbS}_3$  appears to gradually undergo irreversible transformations which decrease the amount of sodium that can be reversibly inserted.  $\text{TaS}_3$  was found to be more stable. The transformations induced in the trisulfides by electrochemical titration with sodium are discussed in terms of the structural and chemical bonding properties of these materials.

Compounds that can react with alkali metals with a large free energy of reaction are potentially useful for battery applications (1, 2). The requirement that the process be readily reversible has put a premium on these reactions (called topochemical), which occur without appreciably modifying either the structure or the chemical bonding of the host material.<sup>1</sup> Typical examples are the layered transition-metal disulfides in which alkali metals are inserted between the weakly bonded layers of the compound (1). Because these intercalation compounds usually form nonstoichiometric phases with a wide compositional range, their energy density is large.

Many efforts have been devoted to finding other materials which meet the reversibility requirements, but for which the reaction product contains a ratio of alkali metal to transition metal of 2 or 3 in order to achieve larger energy densities (3). It was recognized early that materials such as  $\text{TiS}_3$  and  $\text{NbSe}_3$  could incorporate up to three lithium atoms per formula unit (4, 5). However, it was found that only about one-third of the lithium incorporated in  $\text{TiS}_3$  could be removed (6). The reaction was found to be reversible in  $\text{NbSe}_3$ , but although its volumetric energy density was large, its gravimetric energy density was comparable so that of  $\text{TiS}_2$  (7). Past studies have not fully explained why different trichalcogenides show different degrees of reversibility for the reaction with lithium. Tests of the charge/discharge behavior of these compounds under galvanostatic conditions have indicated that the reaction with lithium is more complex than a topochemical reaction and induced structural transformations in the host materials. Unfortunately, x-ray diffraction measurements of the reacted trichalcogenides have typically shown patterns of weak and broad lines which hamper the complete identification of the reaction products.

In this paper we report electrochemical studies on the effects produced by the insertion of sodium in the trisulfides of titanium, niobium, and tantalum. The reaction was carried out by electrochemical titration in high-temperature sodium cells which utilize the solid electrolyte  $\beta'$ -alumina (8). Because  $\beta'$ -alumina is stable in the potential range of the experiment, we have been able to study the process without interference from side reactions with the electrolyte, and in addition we have avoided the problem of electrolyte cointercalation. We discuss how cyclic voltammetry measurements allow us to detect the occurrence of phase transformations in the electrode material with higher sensitivity than possible with conventional galvanostatic measurements. We also show that the reaction products for  $\text{TiS}_3$  can be identified with this technique.

The electrochemical behavior of the trisulfides in sodium cells is shown to be profoundly different from that of the corresponding disulfides because sodium strongly interacts with the polysulfide group  $(\text{S}_2)^{-2}$ , which is characteristic in these materials. Our cyclic voltammetry data indicate that structural and chemical transformations oc-

cur in these materials, but the effects are dissimilar in each compound. XPS measurements of the sulfur 2p core level for the trisulfides are reported which indicate that the sulfur bonding characteristics in  $\text{TaS}_3$  may be different from those of  $\text{TiS}_3$  and  $\text{NbS}_3$ . The observed chemical bonding differences can be correlated with the different behavior of the trisulfides upon electrochemical titration with sodium.

## Sample Preparation

Titanium trisulfide was prepared by direct reaction between sulfur granules (Asarco) and titanium powders (Cerac mesh -325) in sealed quartz ampuls. A small sulfur excess above the stoichiometric composition was used. The ampul was then inserted in a two-zone furnace. The temperatures in the two zones were adjusted so that one end of the ampul was kept at 440°C to avoid high sulfur vapor pressure, and the other end with the metal powders was kept at 560°C. Formation of the undesired disulfide phase was observed if the reaction was carried above 570°C. When the powders had reacted, the temperature of the colder zone was raised to 500°C and the material was annealed for three days. The ampul was then cooled slowly, maintaining the temperature gradient to deposit the small excess sulfur at one end. In this way, blue-gray ribbons of  $\text{TiS}_3$  were obtained, and the largest were roughly 1 cm long and 0.5 mm wide.

$\text{NbS}_3$  and  $\text{TaS}_3$  were prepared in a similar way, starting with Cerac metal powders of -325 mesh. The temperature in the reaction zone was kept at 600°C for  $\text{NbS}_3$  and at 650°C for  $\text{TaS}_3$ , while the cold zone was maintained at 440°C in both cases.  $\text{TaS}_3$  grew as a light felt of fine and short fibers which filled the inside of the ampul.  $\text{NbS}_3$  also grew as fine needles, but with excess sulfur we were also able to obtain long, flat ribbons, similar to  $\text{TiS}_3$ . The lattice constants of the synthesized trisulfides were derived by x-ray diffraction analysis of powder samples and were found to be in agreement with the data in the literature.

## Experimental

The cells used for the electrochemical experiments were made of alumina tubing at the end of which a disk of  $\beta'$ -alumina was sealed with a soft glass. The other end of the ceramic tubing had a ceramic-to-glass transition so that sodium could be vacuum distilled in the container and sealed off. The temperature of the cell was measured with a shielded thermocouple sealed in the sodium compartment, with its tip close to, but not touching, the  $\beta'$ -alumina disk.

The positive electrode was made by pressing transition-metal sulfide fibers on a disk of thin aluminum foil with a die. Upon pressing, the fibers became a compacted felt with a geometrical surface area of 0.1-0.2 cm<sup>2</sup>. The felt stuck slightly to the aluminum foil, which made the handling of the electrode easier. Typically, a few tenths of a milligram of active material were used for the electrode.

The precise amount was determined with an electronic balance by weight difference between the aluminum substrate alone and the pressed electrode. The electrode was then put in the center of a flexible aluminum cup which fitted the ceramic half-cell so that it could be easily positioned against the electrolyte. Contact between the solid electrode and the electrolyte was achieved by slightly pressing the aluminum cup with a flat, rigid cup holder. To apply the pressure, the ceramic half-cell was rigidly mounted by means of a metallic collar into one end of a threaded cylinder made of steel. A spring-loaded plunger was then screwed into the other end of the cylinder so that it pushed the cup holder. A pin was machined in the back of the cup holder to act as a point of contact with the plunger to compensate for the lack of parallelism between the  $\beta$ -alumina disk, cup holder, and plunger. In addition, to improve the contact between the sulfide electrode and the solid electrolyte, a pellet of graphite powders, slightly pressed into a 1 mm-thick disk, was added between the aluminum cup and the flat cup holder. When the pressure was applied, the graphite pellet flowed and pressed the electrode uniformly against the solid electrolyte. With this procedure of mounting the electrode, we were able to obtain an electrode-electrolyte interface with reproducible characteristics, as was demonstrated by the very good reproducibility of the data from sample to sample. At the temperature of operation (less than 320°C), we did not observe any reaction between the sulfide and the aluminum substrate. The cells were assembled and tested in a dry box. The cell assembly was heated in a cylindrical heater whose temperature was regulated within  $\pm 1^\circ\text{C}$ .

The measurements were carried out using PAR electrochemical instrumentation (Model 173 potentiostat, Model 371 coulometer, Model 175 programmer) controlled by a Tektronix 4051 computer. Sodium was inserted in the sulfide electrode and removed from it by discharging and charging the cell at low rates. The charge measured during the electrochemical titration is proportional to the amount of sodium inserted in the electrode material because no side reactions, such as reduction of the electrolyte, occur, and nonfaradaic effects, such as double-layer charging, are very small. These assumptions were verified in our case by changing the thickness of the electrode.

The reaction was carried out under the condition that the voltage of the cell should change at a constant rate with time. Thus, the titration current was observed to increase and decrease as a function of the voltage. The rate of the reaction, monitored by the current, was kept low enough to insure quasi-equilibrium conditions throughout the test. Specifically, the concentration gradients in the particles which compose the electrode were kept small so that the lineshapes of the voltammograms would not become broad and distorted. The use of microelectrodes has the advantage of keeping the time of the experiments relatively short. Because the geometry of the cell did not allow the addition of a reference electrode, the sodium electrode was used as both a counter and a reference electrode. This configuration did not introduce a large error, because the polarization of the sodium electrode was low. This was verified by current step measurements using a sodium/ $\beta$ -alumina/sodium cell. The IR drop of the sulfide cells was also checked with the same technique and found to be less than 20 mV at currents up to 1 mA.

The XPS spectra were obtained with a Vacuum Generator ESCA 3 system using a magnesium anode x-ray source (1253.6 eV). The instrument was operated in the constant pass energy mode with a typical resolution of 1.1 eV full width at half maximum peak height on the Au 4f<sub>7/2</sub> line.

### Results

We report in Fig. 1 the results of the first and second scan for  $\text{TiS}_3$  obtained at 280°C. In this experiment the electrode was 0.3 mg and the scan rate was 0.1 mV/s. On

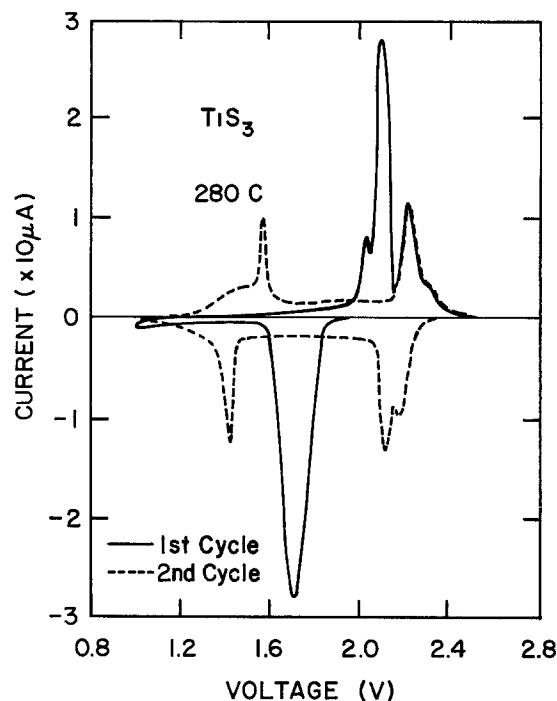


Fig. 1. Cyclic voltammetry curves for a  $\text{TiS}_3$  electrode at a sweep rate of 0.1 mV/s. The negative curves correspond to the insertion of sodium in the electrode, the positive curves to its removal. The solid and dashed lines correspond to the first and second cycles, respectively.

discharge (cathodic wave), a broad current peak appears at 1.7V. The integrated current indicates that the process involves two electrodes per molecule. Below approximately 1.2V, the background current increases slowly. On charge (anodic wave), a complex lineshape, made of four peaks, is observed between 2.0 and 2.4V. The measured titration charge indicates that at least 95% of the sodium inserted in the electrode is removed on charge. Lower coulomb efficiency is observed if the cathodic scan is extended beyond 1V. The second scan is, however, different. Three cathodic peaks are observed at 2.2, 2.1, and 1.4V, respectively. Corresponding peaks, with very similar lineshapes, are observed in the anodic scan shifted by 80 mV toward higher energies. These peaks are the characteristic features observed for  $\text{TiS}_2$ . Similarly, the total charge measured during the second intercalation cycle is equivalent to only a one-electron process, and intercalation is reversible. Subsequent scans give identical results. After the cyclic voltammetry tests, the cell was opened to inspect the electrode. In the case in which the electrode was taken out after a full charge cycle, the color of the electrode was gold. Inspection under an optical microscope revealed that the electrode was now a compacted powder and had lost its originally fibrous appearance. X-ray diffraction data revealed some of the characteristic lines for  $\text{TiS}_2$ , although they were very broad. In another test, a  $\text{TiS}_3$  electrode was removed from a cell after the first discharge to 1.2V. Its color was dark gray black. Part of the electrode was enclosed in a glass capillary for x-ray diffraction analysis while still in the dry box. Only a few broad lines were observed from which it was not possible to identify the reaction products.

The cyclic voltammetry curves for niobium and tantalum trisulfides show different features. In Fig. 2 we report the first and sixteenth complete scans for a  $\text{NbS}_3$  electrode of 0.3 mg, and part of the second. The voltammograms were obtained at 280°C and at a scan rate of 0.1 mV/s. The first discharge curve shows a large current peak at 1.7V, similar to that observed for  $\text{TiS}_3$ , but narrower. The charge corresponding to the peak indicates a two-electron reduction process. At 0.9V, another peak corresponding to a one-electron process is observed. In the subsequent charge scan, a peak is observed at 1.5V, a doublet appears at 2.1-2.2V, and a small peak can be seen at 2.4V. The coulomb efficiency during the first cycle is

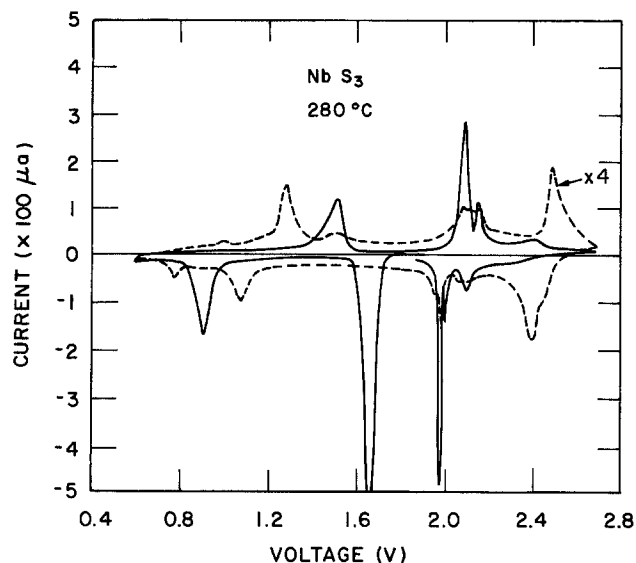


Fig. 2. Cyclic voltammograms for a  $\text{NbS}_3$  electrode at a sweep rate of 0.1 mV/s. The solid and dashed lines correspond to the first and sixteenth cycles, respectively.

about 90%. Although the lineshape of the first cathodic voltammogram is quite different from that of the first anodic voltammogram, on subsequent cycles the cathodic and anodic curves become more symmetrical. To illustrate this point, the first part of the second voltammogram is included in Fig. 2. Three peaks appear at 1.95, 2.10, and 2.34V, respectively, which are similar to the peaks observed in the first anodic scan. Quite different behavior is observed for the peak at lower voltages. In fact, the cathodic peak splits into two components, which grow at 0.8 and 1.1V, respectively, and have a 2:1 intensity ratio. The anodic peak at 1.5V instead starts decreasing in intensity, and another peak starts growing at 1.3V. The total charge associated with these peaks decreases monotonically and after a few cycles is roughly  $0.5 e^-/\text{NbS}_3$ . At higher voltages, the weak peaks at 2.4V in the cathodic scan and at 2.5V in the anodic scan gradually increase in intensity, while the other two peaks become weaker. By the tenth cycle, the total charge measured during a discharge cycle was  $1.5 e^-/\text{mol}$  and kept decreasing. Separate scans over either the 0.6-1.6V or 2.0-2.7V region gave similar results, indicating that the processes are independent.

In Fig. 3 we show the first and eighth complete scans for a  $\text{TaS}_3$  electrode taken at 280°C. Part of the second scan is also shown. The scan rate was 0.1 mV/s and the weight of the electrode was 0.4 mg. A peak at 1.7V and a small peak at 1.9V are observed on the first discharge. The total integrated current indicates a two-electron process. Another peak, corresponding to a one-electron process, is observed at 0.6V. On charge, two peaks appear at 1.0 and 1.3V respectively, and a very broad feature, which appears to be made of at least three components, is observed to be centered at 2.3V. The coulomb efficiency of the first cycle is about 95%. On the second discharge an asymmetric peak appears at 2.1V. This peak shifts on subsequent scans by 100 mV to higher voltages, splitting into two components of 3:1 intensity ratio. After a few cycles, the peak lineshape remains constant. During the transformation, the charge associated with the higher voltage processes decreases by 20%. The lower peak instead shifts by 50 mV to lower voltages, increasing its intensity, so that the total charge measured during the entire scan remains constant within 1-2%. The peaks in the anodic waves change to become more symmetrical with the cathodic peaks. The peak at 1.3V disappears and the one at 0.9V becomes stronger. The peak lineshape near 2.2V becomes sharper as if the central component grew at the expense of the others. Although the cyclic voltammograms measured for  $\text{TaS}_3$  showed lineshape transformations similar to those observed for  $\text{NbS}_3$ , the two compounds

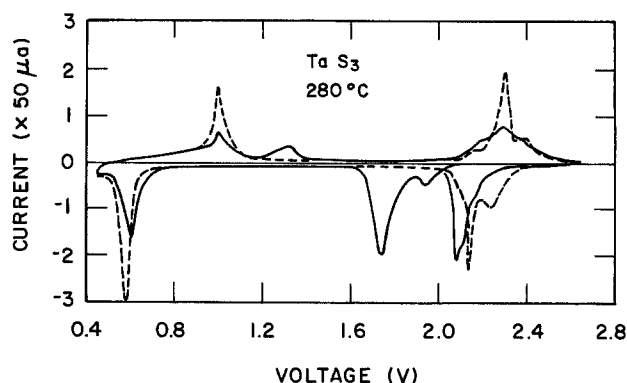


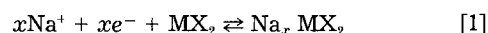
Fig. 3. Cyclic voltammograms for a  $\text{TaS}_3$  electrode at a sweep rate of 0.1 mV/s. The solid and dashed lines correspond to the first and eighth cycles, respectively.

behave differently in the following respects. First, in  $\text{TaS}_3$ , the lineshape modifications occur without substantial loss in electrode utilization and coulomb efficiency. Second, the  $\text{TaS}_3$  peaks change their intensity, but they do not shift substantially in voltage. And last, the changes in  $\text{TaS}_3$  occur within the first three or four cycles, after which subsequent voltammograms do not change appreciably.

The  $\text{NbS}_3$  and  $\text{TaS}_3$  electrodes did not seem to have lost their fibrous appearance after the electrochemical tests, at least under low optical magnification. They did seem, however, to react with air, probably due to the remaining sodium that cannot be removed from the material during the electrochemical titration. X-ray diffraction measurements were performed on pieces of fully charged electrodes after they had been cycled several times. The samples were sealed in glass capillary while still in the dry box to prevent reaction with air. Their diffraction patterns showed only a few broad lines, suggesting that both materials had become highly disordered during the reaction. The presence of disulfide or trisulfide species could not be conclusively demonstrated.

### Discussion

Our cyclic voltammetry results demonstrate that the effects produced by the insertion of sodium in  $\text{TiS}_3$ ,  $\text{NbS}_3$ , and  $\text{TaS}_3$  are more complex than those observed in the disulfides (10). Titration of layered dichalcogenides with alkali metals has been shown to produce ternary phases according to the equation



where M is the transition metal and X is either sulfur or selenium. Stoichiometric and nonstoichiometric reaction products have been reported for the disulfides (12). The redox process described by Eq. [1] does not have a simple Nernstian behavior because it involves solid-state species. Typically, the equilibrium voltage of the titration cell is not a linear function of the alkali-metal concentration in the electrode material, and it changes discontinuously when a new phase is formed during the process. These discontinuities are resolved with the cyclic voltammetry technique, with much higher sensitivity than possible with galvanostatic measurements, because this method, at very low rates, is equivalent to a differential measurement of the curve representing the sodium concentration in the electrode as a function of its equilibrium voltage. Thus, current peaks are observed when the free energy of reaction changes and can be correlated with changes in the electroaffinity of the host material, with changes in the site occupied by sodium and/or with structural transformations of the ternary compound formed during the process. In particular, very sharp current peaks are seen when two phases coexist. Conversely, the current is approximately constant when the reaction produces a homogeneous phase such as a solid solution (10).

We previously reported voltammograms for  $\text{TiS}_2$ ,  $\text{NbS}_2$ , and  $\text{TaS}_2$  obtained with the same cell configuration and

using microelectrodes (10). For each of the disulfides, we observed characteristic current peaks which did not appreciably change upon cycling. In addition, the cathodic and anodic waves were fairly symmetrical. We discussed how these features are characteristic for an intercalation process which affects the stacking of the disulfide layers but not their chemical bonding. The voltammograms for the trisulfides instead show modifications in lineshape and shifts in peak position as a function of cycling, which indicates that profound structural modifications occur during the reaction with sodium.

Before discussing the electrochemical data, it is useful to summarize the structural and chemical bonding properties of the materials under study. The structure of these trisulfides can be regarded as being built with chains of sulfur trigonal prisms, stacked to share their triangular faces, with the metal at the center of each prism. To satisfy the valence rules, sulfur-sulfur bonds are formed in such a way that two anions in each unit become paired (11). The chains are alternatively displaced along their axis by half a prism length. Their relative distance is such that the separation between the metal in one chain and one sulfur from each of the two adjacent chains is similar to the intrachain metal-sulfur distance. As a consequence, the metal becomes eightfold coordinated, and the resulting cross linking produces slabs of coupled chains. The slabs are weakly bonded by van der Waals forces because sulfur pairs form their outer layers and thus, the materials are pseudo two-dimensional. Details of intrachain or interchain interactions differ from one compound to another, giving rise to different layering patterns and different unit cells. While in  $\text{TiS}_3$  (13) and  $\text{NbS}_3$  (14), the chains are all equal and the unit cell contains two columns; the orthorhombic polytype of  $\text{TaS}_3$  (15) has a more complicated unit cell, containing 24 chains. Although the structure of orthorhombic  $\text{TaS}_3$  has not yet been exactly determined, it has been proposed that it contains several types of chains that differ from one another by the degree to which sulfur atoms are paired. The presence of such inequivalent chains has been determined in similar compounds, such as  $\text{TaSe}_3$  and  $\text{NbSe}_3$  (11), and in the less common monoclinic polytype of  $\text{TaS}_3$  (16), which can be obtained at high pressure. In addition, when the anion-anion pairing is relaxed, interchain anion bonding occurs. As a result, the slabs formed by cross-linked chains become somewhat puckered, making the van der Waals gap less defined (11).

One important structural characteristic of these trisulfides is the presence of sulfur-sulfur bonds. This pair is usually referred to as the polysulfide group, because x-ray diffraction studies in  $\text{TiS}_3$  and  $\text{NbS}_3$  have shown that this bond length is equivalent to that found in other known polysulfides. Therefore, the trisulfides have been formally described by the ionic formula  $\{\text{M}^{+4}(\text{S}_2)^{-2} \text{S}^{-2}\}$ , although they are mostly covalently bonded. We also have verified with XPS measurements the presence of sulfur in different bonding configurations (17). In Fig. 4 we show the XPS spectra of the sulfur 2p core level that we measured for  $\text{TiS}_3$ ,  $\text{NbS}_3$ , and orthorhombic  $\text{TaS}_3$ . The spectra for  $\text{TiS}_3$  and  $\text{NbS}_3$  can be decomposed into two doublets. Each doublet corresponds to the 3/2 and 1/2 spin-orbit split components of the 2p core level. The intensity ratio between the two doublets is 2:1, the more intense one being at higher binding energies. This indicates that less charge is localized on the more abundant species, as suggested by the ionic formula of the compound. In contrast, the lineshape observed for  $\text{TaS}_3$  cannot be decomposed into only two components, suggesting a more complex bonding configuration as indicated by x-ray diffraction studies.

We have observed pronounced differences in the lineshapes of the voltammograms of the trisulfides and in the behavior of their voltammograms upon cycling. However, it is possible to identify one common feature: on first discharge, the three materials all undergo a two-electron reduction process at approximately the same potential. We associate this process with the reduction of the

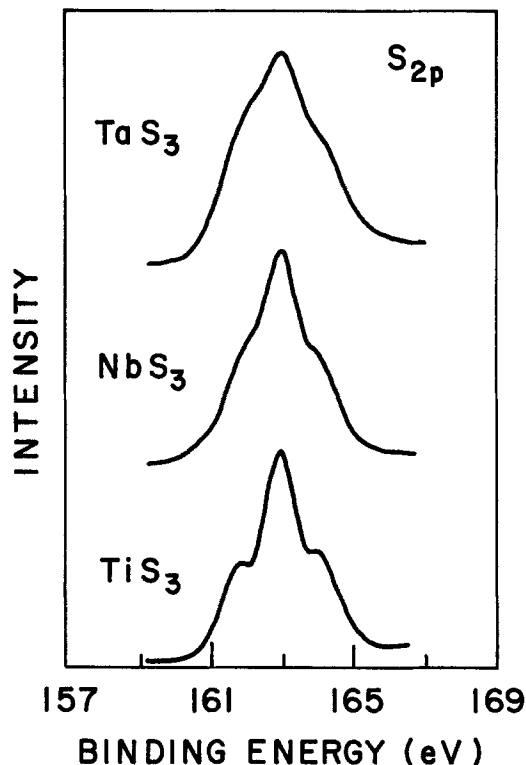


Fig. 4. XPS spectra of the  $\text{S}_{2p}$  core level for  $\text{TiS}_3$ ,  $\text{NbS}_3$ , and  $\text{TaS}_3$ .

polysulfide group with concomitant insertion of 2 Na/unit. It seems likely that sodium diffuses into the van der Waals gap of the material, although we were unable to confirm from our x-ray diffraction data that the unit cell expands along only one direction during this process. The initial reduction process breaks the polysulfide bond and produces different effects in each compound. For example,  $\text{TiS}_3$  becomes unstable because the trigonal prismatic coordination of the cation is stabilized by the sulfur pair. Once the pair is broken, the structure tends to assume the more stable octahedral coordination which is found in  $\text{TiS}_2$  (18). The disproportionation of  $\text{TiS}_3$  to  $\text{TiS}_2$  is clearly demonstrated by the cyclic voltammetry results because the curves obtained for scans subsequent to the first one are the same as the ones obtained for  $\text{TiS}_2$ . It could be argued that the formation of  $\text{TiS}_2$  occurs when the polysulfide is oxidized and the sodium is removed from the compound, because during the first anodic cycle, the characteristic disulfide peak at 1.5V is missing, while the peak at 2.1V is present. Moreover, because all of the sodium is removed during the first charge and the first oxidation peak is found above 2.0V, it seems unlikely that sodium sulfide and titanium disulfide are formed during the first discharge. The few broad lines observed in the x-ray diffraction pattern of an electrode discharged to 1.2V did not seem to correlate with those expected for  $\text{Na}_2\text{S}$ . It should be noticed that in the voltammograms of  $\text{TiS}_3$ , the two peaks at 2.1V are resolved, indicating that the particle size of the product is small and that the disulfide is stoichiometric. Either excess of titanium or large particle size have the effect of broadening the peak linewidths. The spectra do not show any feature that can be associated with the presence of free sulfur liberated after the first cycle. However, a faint yellow deposit could be seen at the edge of the alumina disk after opening the cell. The absence of electrochemical activity from the free sulfur may be due to a loss of electrical contact. Because the quantity of sulfur is small, it is possible that it evaporates away during the experiment due to the relatively high temperature. We checked the transformation into the disulfide's not just being caused by the high temperature. A fresh electrode was kept at 300°C in a cell in open-circuit conditions for several days before being cycled, and it showed the same behavior.

Contrasting with the behavior of  $\text{TiS}_3$ , no abrupt loss of capacity is observed in  $\text{NbS}_3$  and  $\text{TaS}_3$  after the first cycle. In both materials, the peaks in the first anodic scan and second cathodic scan above 2V are fairly symmetric, and the corresponding charge is greater than  $1.5 e^-/\text{mol}$ , indicating that the redox process is still associated with a polysulfide species. It also seems unlikely that the cation should change coordination, because the trigonal prismatic coordination is more stable than the octahedral one, at least in both niobium and tantalum disulfides (18). In addition, in all the scans these materials show another well-defined reduction process at voltages lower than 1V, not observed in  $\text{TiS}_3$ . It is tempting to associate the low-voltage redox process with the oxidation and reduction of the cation. However, the trisulfides are largely covalent, and their atomic orbitals are well hybridized, so assignment of a specific valence state to the cation is purely formal. It could also be argued that  $\text{TiS}_3$  can be further reduced below 1V because the titration current increases below this voltage. This process is, however, irreversible, because the anodic current is very small below  $\sim 1.7\text{V}$ , suggesting that sodium sulfide may be formed below 1V.

For the case of  $\text{NbS}_3$ , our results suggest that this material undergoes irreversible transformations upon reaction with sodium.  $\text{NbS}_3$  appears to transform slowly under repeated cycling, because new peaks in the voltammograms become more prominent and the electrode utilization decreases within ten cycles to almost half of its first-cycle value. However, the possibility that  $\text{NbS}_3$  disproportionates to the disulfide seems contradicted by the fact that, even after fifteen cycles, the material can be inserted with more than 1 Na/Nb. The large sodium capacity would indicate that the polysulfide bond is still involved in the redox process, because the disulfides are typically found to reversibly incorporate 1 Na/unit at most (10). The lineshape of the voltammograms, even after several cycles, is different from that measured for rhombohedral  $\text{NbS}_2$  (10). It should be noticed, however, that several nonstoichiometric phases have been identified in the sulfur-niobium phase diagram (19) and that their behavior in sodium cells has not been determined. Peculiar to  $\text{NbS}_3$  is the very sharp peak at 1.95V, which is a characteristic potential for polysulfide reduction. The intensity of this peak decreases rapidly with cycling, while the peak at 2.4V increases to a comparable intensity. This feature might indicate that a disulfide phase is being formed at the expense of the trisulfide, because the typical potentials observed for sodium intercalation in the disulfides range between 2.2 and 2.4V, and the lineshape of the peak at 2.4V is similar to that observed for intercalation in those compounds (10). X-ray diffraction measurements on a fully charged electrode after sixteen charge/discharge cycles showed only a few diffuse lines from which the reaction products could not be identified.

$\text{TaS}_3$  is the most stable of the three sulfides. After the first few cycles, sodium seems to be inserted and removed from this compound with little loss in the electrode capacity, as is typically observed in an intercalation reaction. We suggest that the greater stability of  $\text{TaS}_3$  when compared to the other two trisulfides may be related to the presence of relaxed sulfur pairs. The occurrence of relaxed polysulfide groups could be attributed to an increased charge transfer from the cation to the anion as if tantalum prefers the pentavalent configuration (16). Relaxation of intrachain sulfur-sulfur bonds may also promote interchain chalcogen interactions as it is observed, for instance, in  $\text{TaSe}_3$  (11). Thus, the reduction process at high voltage may be quite complex, involving either different sulfide species or the compound as a whole. It should be noted, in fact, that the line shape of the peak above 2V is asymmetrical and is quite different from that observed for  $\text{TiS}_3$  and  $\text{NbS}_3$ . In addition, after several cycles, the charge associated with the lower redox process is found to be larger than  $1 e^-/\text{Ta}$ , suggesting the presence of pentavalent cations. Some degree of electrochemical irreversibility is present in the behavior of the

material because the anodic and cathodic peaks are widely separated. In particular, the peaks at low voltages are shifted by 400 mV. A large peak separation could result if the cation ligand field is distorted during the reduction process so that the oxidation potential is shifted to higher values.

The energy density of the  $\text{TaS}_3$  electrode alone extrapolated from the tenth cycle is about 350 Wh/kg, which is similar to the one found for  $\text{TiS}_2$  in a similar sodium cell (360 Wh/kg) (9). Because the density of  $\text{TaS}_3$  is almost twice as large as that of  $\text{TiS}_2$ , the utilization of  $\text{TaS}_3$  could be more advantageous in applications in which the volumetric energy density needs to be high. In addition, the fibrous morphology of  $\text{TaS}_3$  makes it easier than for the platelet-like disulfide materials to construct high surface-area electrodes which have good mechanical integrity.

Some of the trisulfides have been tested in the past as electrode materials in room-temperature lithium cells, but no tests have been performed in sodium cells.  $\text{TiS}_3$  and  $\text{NbS}_3$  showed poor reversibility with lithium (1, 20). It was found that three equivalents of lithium could be inserted electrochemically in 1 mol of  $\text{TiS}_3$ , but that less than 1 eq/mol could be removed at very low current rates. The lack of reversibility observed in the galvanostatic charge/discharge data was ascribed to the formation of lithium sulfide and titanium disulfide (1). However, neither x-ray data nor the electrochemical data could conclusively show the presence of either compound. Similarly, it was found that 2.6 eq/mol of lithium could be inserted in  $\text{NbS}_3$  on first discharge, only 80% of which could be removed (20). Our electrochemical data seem to indicate that no sodium sulfide is formed in the trisulfides during the first electrochemical discharge. We also found in our experiments that sodium can be removed from both  $\text{TiS}_3$  and  $\text{NbS}_3$  after the first discharge in much larger percentage than that measured in the case of titration with lithium. The greater degree of rechargeability observed in our experiments is probably due to the higher temperature of operation, instead of being related to intrinsically different effects occurring from the two alkali metals. In fact, it was shown in our earlier results that  $\text{TiS}_3$  in a similar high-temperature sodium cell was much more reversible and had a deeper discharge range than in room-temperature sodium cells with a liquid electrolyte (9, 21). There are no data in the literature about the behavior of  $\text{TaS}_3$  electrodes in lithium cells. Because in our experiments this compound is found to be rechargeable, it is possible that it may also have good rechargeability characteristics in room-temperature lithium cells, as was found for  $\text{NbSe}_3$  (7). This material can be reversibly titrated with three equivalents of lithium per mole, and under galvanostatic discharge, it exhibits two plateaus. We found in our sodium cells that  $\text{NbSe}_3$  behaves similarly to  $\text{TaS}_3$  (22). In particular, three equivalents of sodium can be inserted in one mole of  $\text{NbSe}_3$  and removed from it; the material can be cycled several times with little loss in electrode capacity, and only small changes in the voltammograms occur after repeated cycling. However, three separate redox processes seem to occur in  $\text{NbSe}_3$  after the first cathodic scan.  $\text{NbSe}_3$  was found to contain three kinds of chains which differ by the degree of anion pairing (11). These similarities between  $\text{TaS}_3$  and  $\text{NbSe}_3$  seem to point out that the characteristics of the anion bonding in the trichalcogenides may be the important factors in determining their stability toward the insertion of alkali metals.

### Conclusion

We have shown that the electrochemical behavior of the trisulfides of titanium, niobium, and tantalum is dominated by the redox process on the polysulfide group. As a consequence, irreversible transformations are induced in the trisulfides, unlike what is observed in the corresponding disulfides. Although the trisulfides have similar structural characteristics, some differences in their bonding properties can be identified. We suggest that the different degrees of stability toward insertion of sodium

observed in these compounds are a consequence of different sulfur-sulfur bonding configurations. Our voltammograms clearly show the disproportionation of  $TiS_3$  into the corresponding disulfide. It is not possible, on the basis of our data, to identify the precise mechanisms by which  $NbS_3$  loses electrode capacity, although decomposition to the disulfide cannot be ruled out. The electrochemical behavior of  $TaS_3$  instead resembles more what is expected for an intercalation process: only small changes are observed in its voltammograms upon cycling.  $TaS_3$  may be potentially useful as an electrode material for applications in which a high volumetric energy density is required.

#### Acknowledgments

The author is deeply indebted to G. J. Tennenhouse for many helpful discussions and for providing the  $\beta''$ -alumina disks. The help of J. E. deVries in the XPS data acquisition and the assistance of F. R. Runkle in making the ceramic cells are gratefully acknowledged.

Manuscript submitted Jan. 13, 1984; revised manuscript received Sept. 12, 1984.

Ford Motor Company assisted in meeting the publication costs of this article.

#### REFERENCES

1. M. S. Whittingham, *This Journal*, **123**, 315 (1976).
2. D. W. Murphy and F. A. Trumbore, *J. Cryst. Growth*, **39**, 185 (1977).
3. K. M. Abraham, *J. Power Sources*, **7**, 1 (1981).
4. R. R. Chianelli and M. B. Dines, *Inorg. Chem.*, **14**, 2417 (1975).
5. D. W. Murphy and F. A. Trumbore, *This Journal*, **123**, 960 (1976).
6. G. L. Holleck and J. R. Driscoll, *Electrochim. Acta*, **22**, 647 (1977).
7. J. N. Carides and D. W. Murphy, *This Journal*, **124**, 1309 (1977).
8. J. T. Kummer and N. Weber, *S. A. E. Trans.*, **26**, 1003 (1968).
9. M. Zanini, J. L. Shaw, and G. J. Tennenhouse, *This Journal*, **128**, 1647 (1981).
10. M. Zanini, J. L. Shaw, and G. J. Tennenhouse, *Solid State Ion.*, **5**, 371 (1981).
11. F. Hulliger, in "Physics and Chemistry of Materials with Layered Structures," Vol. 5, F. Levy, Editor, Reidel (1976).
12. M. S. Whittingham, *Solid State Chem.*, **12**, 41 (1978).
13. F. K. Mctaggart and A. D. Wadsley, *Aust. J. Chem.*, **11**, 445 (1958); S. Furuseth, L. Brattas, and A. Kjekshus, *Acta Chem. Scand.*, **A29**, 623 (1975).
14. J. Rijnsdorp and F. Jellinek, *J. Solid State Chem.*, **25**, 325 (1978).
15. E. Bjerkelund and A. Kjekshus, *Z. Anorg. Allg. Chem.*, **328**, 235 (1964); A. Bjerkelund, J. H. Femor, and A. Kjekshus, *Acta Chem. Scand.*, **20**, 1836 (1966).
16. A. Meerschaut, L. Guemas, and J. Rouxel, *J. Solid State Chem.*, **36**, 118 (1981).
17. M. Zanini and J. E. deVries, Internal Report, Ford Motor Company (1983).
18. F. R. Gamble, *J. Solid State Chem.*, **9**, 358 (1974).
19. F. Kadijk and F. Jellinek, *J. Less Common Metals*, **19**, 421 (1969).
20. G. L. Holleck, F. S. Shuker, and S. B. Brummer, Proceedings 10th IECEC, Newark, Delaware (1975).
21. G. H. Newman and L. P. Klemann, *This Journal*, **127**, 2097 (1980); K. M. Abraham, L. Pitts, and R. Schiff, *ibid.*, **127**, 2545 (1980).
22. M. Zanini, Unpublished results.

## The Photoelectrochemical Behavior of $CuIn_5S_8$

B. Scrosati\* and L. Fornarini

Department of Chemistry, University of Rome, 00185 Rome, Italy

G. Razzini and L. Peraldo Bicelli\*

Department of Applied Physical Chemistry, The Milan Polytechnic, Research Centre on Electrode Processes of the CNR, 20133 Milan, Italy

#### ABSTRACT

The photoelectrochemical behavior of  $n-CuIn_5S_8$ , a chalcogenide having a spinel-type structure, has been studied in various electrolytes by measuring the spectral response, the current-potential characteristics, and the differential capacitance. The best results have been obtained in an aqueous sulfide-polysulfide solution, where the  $CuIn_5S_8$  semiconductor electrode shows an excellent stability. The flatband potential of this semiconductor electrode has been found to depend on the solution composition. The most negative values have been observed in the sulfide-polysulfide solution, owing to specific adsorption of  $S^{2-}$  ions on the electrode surface. Preliminary results on the output power characteristic of the  $CuIn_5S_8$  photoelectrochemical cell are also discussed.

Progress in the development of photoelectrochemical cells has required the investigation of new semiconductor electrodes exhibiting a good stability against photodecomposition and a high absorption in the visible portion of the solar spectrum. Some ternary semiconducting compounds have been shown to satisfy the above conditions, and, in particular, analogues of II-VI compounds, obtained by cross-substitution of the electropositive constituent, have lately been the subject of growing scientific interest.

In this work, we report the photoelectrochemical performance of  $CuIn_5S_8$ , whose optical and electrical properties are known (1). This  $n$ -type semiconductor has a cubic spinel-type structure similar to that of  $CdIn_2S_4$  (2).

The ideal spinel structure can be viewed as a cubic close-packed partial structure of anions in which one-

eighth of the tetrahedral and one-half of the octahedral sites are occupied by cations.

Considering the general formula  $M_{1/2}^{+}M_{1/2}^{3+}[M_2^{3+}]X_4^{2-}$  of a normal 1-3 spinel where the cations in the brackets occupy octahedral sites and the remaining cations occupy tetrahedral sites,  $CuIn_5S_8$  may be written as  $Cu_{1/2}In_{1/2}[In_2]S_4$ . This formula can also be deduced by substituting monovalent copper cations and trivalent indium cations for divalent cadmium cations in  $CdIn_2S_4$ , which is, however, a partial inverse thio-spinel:  $Cd_{1/2}In_{1/2}(Cd_{1/2}In_{3/2})S_4$  (3).

$CuIn_5S_8$  crystallizes in the space group  $F\bar{4}3m$  ( $T^h_d$ ), has a cubic structure with lattice dimension  $a = 10.6858\text{\AA}$  and has eight molecules per unit cell (4). Moreover, according to complete x-ray structural determinations, the tetrahedral sites are split into two nonequivalent groups with an unequal distribution of copper and indium ions. In fact, one site is occupied to the extent of 52.4% by cop-

\* Electrochemical Society Active Member.